analytical chemistry

pubs.acs.org/ac Article

5-Hydroxymethylcytosine Glucosylation-Triggered Helicase-Dependent Amplification-Based Fluorescent Biosensor for Sensitive Detection of β-Glucosyltransferase with Zero Background Signal

Meng Liu,[‡] Chen-chen Li,[‡] Xiliang Luo,[*] Fei Ma,[*] and Chun-yang Zhang[*]

Cite This: https://dx.doi.org/10.1021/acs.analchem.0c04382 Read Online

ACCESS | Metrics & More | Article Recommendations | Supporting Information

ABSTRACT: β-glucosyltransferase (β-GT) catalyzes the glucosylation of 5-hydroxymethylcytosine (5-hmC) to enable the survival of bacteriophage and parasite in host cells, and it is a critical tool enzyme for 5-hmC assay. However, few methods are available for β-glucosyltransferase assay, and they usually have the drawbacks of radioactive contamination, high background, laborious procedures, and unsatisfactory sensitivity. Herein, we develop a new fluorescent biosensor with zero background signal for sensitive detection of β-GT activity based on 5-hmC glucosylation-triggered helicase-dependent amplification (HDA). The detection probe we designed may act as both a probe for β-GT recognition and a template for HDA amplification. The β-GT-catalyzed 5-hmC glucosylation can protect the detection probes from both the cleavage by MfeI restrictive enzyme and the digestion by exonucleases I and III. The remaining detection probes can subsequently act as the templates for exponential HDA amplification to generate numerous double-stranded DNA products, which can be easily detected by SYBR Green I in a label-free manner. The zero background can be achieved by efficient elimination of primer−dimer nonspecific amplification and complete digestion of nonglucosylated detection probes. This biosensor exhibits high sensitivity and good specificity, and it can be further used to analyze β-GT kinetic parameters and screen the inhibitors, providing a powerful platform for deeper understanding of β-GT biological functions and promoting β-GT-related epigenetic studies. Furthermore, this biosensor can be extended to detect various DNA-modifying enzymes by simply replacing the recognition sequence and restriction enzyme.

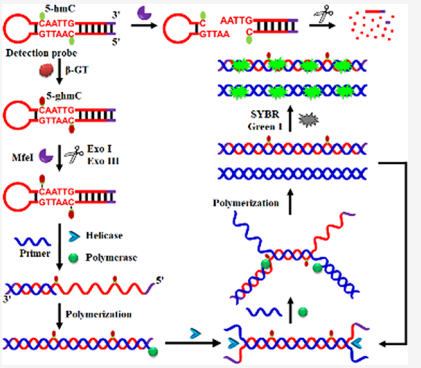

β-glucosyltransferase (β-GT) is a kind of DNA-modifying enzyme with the capability of catalyzing the transfer of β-D-glucosyl residue from uridine diphosphate-α-D-glucose (UDP-glucose) to the hydroxyl group of 5-hydroxymethylcytosine (5-hmC), resulting the formation of glucosylated-5-hmC (5-ghmC).[1−3] In bacteriophage, this β-GT-catalyzed 5-hmC glucosylation is a critical protection mechanism responsible for preventing the bacteriophage's DNA from digestion by nucleases of host bacteria,[4−6] and it is closely linked to the control of gene transcription and expression.[7] In parasite *Trypanosoma brucei*, the β-GT can prevent parasite from immune recognition and neutralization by host cells through the regulation of variant surface glycoprotein (VSG) expression.[8] Besides its fundamental biological roles, β-GT can serve as a critical tool enzyme for 5-hmC assay. Besides A, T, C, G, and 5-methylcytosine (5-mC), the 5-hmC is usually taken as the sixth DNA base[9] with potential roles in DNA demethylation,[10,11] somatic cell reprogramming,[12] embryonic development,[13−16] and disease occurrence.[15,17−21] Nevertheless, the function of 5-hmC is largely unrevealed, one obvious reason is that the abundance of 5-hmC is extremely low (10−100 times lower than 5-mC),[22,23] making it hard to be accurately detected. The β-GT can greatly facilitate the characterization and detection of 5-hmC through the highly selective labeling of target 5-hmC with functional moieties such as radiolabel,[24] biotin,[25] and fluorophore.[26] Therefore, the efficient detection of β-GT activity is of great importance to further revealing its biological functions and promoting 5-hmC-related epigenetic researches.

So far, only a few methods are available for β-GT assay. The conventional methods based on capillary zone electrophoresis[27] and radioisotopic labeling (UDP-[^{14}C]-glucose[27] or UDP-[^{3}H]-glucose[28]) are usually used to detect β-GT activity through the direct monitoring of the enzyme product UDP and 5-ghmC, but the involvement of laborious procedures, sophisticated instruments, and hazardous materials greatly limit their wide applications. Alternatively, some new β-GT biosensors based on electrochemical,[29,30] photoelectrochemical (PEC),[31] and electrochemiluminescent (ECL)[32,33] measure-

Received: October 16, 2020
Accepted: November 24, 2020

ments have been established with low cost, good reproducibility, and high selectivity. Nevertheless, these biosensors require complicated immobilization, washing, and separation steps, suffering from tedious procedures of preparation and functionalization of nanomaterials including magnetic particle,[30] WS_2 nanosheet,[31] gold nanoparticle,[32] and gold nanocluster[33] and exhibiting relatively low sensitivity due to the inherent high background signal and the lack of proper signal amplification strategy. Consequently, the development of simple and sensitive β-GT biosensors is urgently needed.

We report a new fluorescent biosensor for sensitive β-GT activity assay using 5-hmC glucosylation-triggered HDA. HDA is a new nucleic acid signal amplification approach that can achieve more than a million-fold amplification under isothermal conditions.[34,35] The DNA helicase can unwind the dsDNAs to produce the single-stranded DNA templates, initiating the primer hybridization and the subsequent DNA polymerase-catalyzed extension.[34] Superior to the reported polymerase chain reaction,[36] exponential amplification reaction,[37] rolling circle amplification,[38,39] and loop-mediated isothermal amplification,[40,41] the HDA exhibits much simpler reaction scheme and shorter assay time (less than 1 h), and it has been successfully adopted for sensitive detection of nucleic acids,[42,43] proteins,[44] and pathogens.[45] In the proposed biosensor, we exploit HDA for amplified biosensing of β-GT and achieve zero background and highly sensitive β-GT detection. Moreover, this biosensor can be further used to analyze β-GT kinetic parameters and screen the inhibitors.

EXPERIMENTAL SECTION

Materials. All oligonucleotides (Table 1) were obtained from TaKaRa Bio Inc. (Dalian, China) and dissolved to 10 μM with Tris-EDTA buffer solution. Prior to use, 5 μM detection probes with hairpin structure were prepared by incubating in a buffer containing 1.5 mM $MgCl_2$ and 10 mM Tris−HCl (pH 8.0) for 5 min at 95 °C and subsequently cooling to room temperature. The 50× uridine diphosphate glucose (UDP-glucose), β-glucosyltransferase (β-GT), MfeI-HF, exonucleases I and III (*Escherichia coli*), IsoAmp II universal tHDA kit (including helicase and polymerase), *Hha*I, uracil DNA glycosylase (UDG), and alkaline phosphatase (ALP) were bought from New England Biolabs (Ipswich, MA). The uridine 5′-diphosphate disodium salt hydrate and 4-phenylimidazole were purchased from Sigma-Aldrich (St. Louis, MO). The fetal bovine serum (FBS) was bought from Gibco (Grand Island, NY). The SYBR Gold and SYBR Green I were purchased from Life Technologies (Carlsbad, CA). Ultrapure water was obtained from a Millipore filtration system (Temecula, CA).

Table 1. Sequences of the Oligonucleotides[a]

note	sequence (5′−3′)
detection probe	A*G*T ATG GGA CTT TCC GTC TC^{hm}C *AAT TGA* CTA CAG AGA CAG ATA CTT AAT ACT AGT ^{hm}C*AA TTG* GAG ACG GAA AGT CCC ATA *C*T
primer	AGT ATG GGA CTT TCC GTC TCC AAT TGA CTA
C-probe	A*G*T ATG GGA CTT TCC GTC TC*C AAT TGA* CTA CAG AGA CAG ATA CTT AAT ACT AGT *CAA TTG* GAG ACG GAA AGT CCC ATA *C*T
5-mC-probe	A*G*T ATG GGA CTT TCC GTC TC^{m}C *AAT TGA* CTA CAG AGA CAG ATA CTT AAT ACT AGT ^{m}C*AA TTG* GAG ACG GAA AGT CCC ATA *C*T

[a]The asterisk denotes the phosphonothioate modification between deoxyribonucleotides. In the detection probe, the MfeI recognition site is shown in italics.

***β*-GT Detection.** First, 1 μL of β-GT at different concentrations was incubated with 200 nM detection probe in 10 μL of buffer containing 80 μM UDP-glucose, 10 mM magnesium acetate, 50 mM potassium acetate, 20 mM tris-acetate, and 100 μg/mL BSA at 37 °C for 1 h to complete the glucosylation of detection probe. Subsequently, 5 μL of MfeI (60 U) was added and incubated for 4 h at 37 °C. The nonglucosylated detection probes were then digested by Exo III (10 U) and Exo I (10 U) for 30 min at 37 °C. After the termination of nuclease activity by heating at 80 °C for 20 min, the HDA reaction was performed using IsoAmp II universal tHDA kit according to the instruction manual. To improve the assay sensitivity, mix A and mix B were prepared separately, with mix A (25 μL) containing 20 μL of digestion mixture, 0.8 μL of 10 μM primer, and 2.5 μL of 10× annealing buffer II (note: mix A was incubated at 95 °C for 2 min and then placed promptly on ice), and mix B (15 μL) containing 1.6 μL of 100 mM $MgSO_4$, 1.5 μL of 10× annealing buffer II, 2.8 μL of IsoAmp enzyme mix, 2 μL of IsoAmp dNTP solution, 3.2 μL of 500 mM NaCl, and 1× SYBR Green I. The HDA reaction was initiated by mixing mix A (25 μL) and mix B (15 μL). A Bio-Rad CFX connect real-time system was used for real-time fluorescence measurement with intervals of 30 s at 65 °C.

Gel Electrophoresis. The 12% nondenaturing polyacrylamide gel electrophoresis (PAGE) was employed to analyze the detection probe cleavage products in 1× TBE buffer (9 mM boric acid, 9 mM Tris-HCl, 0.2 mM ethylenediaminetetraacetic acid (EDTA), pH 7.9), with the gels being stained by SYBR Gold. The 2% agarose gel electrophoresis was employed to analyze the HDA amplification products in 1× TAE buffer (2 mM EDTA, 40 mM Tris-acetic acid, pH 8.0), with the gels being stained by SYBR Green I. A Bio-Rad ChemiDoc MP Imaging System (Hercules, CA, USA) was used for gel imaging.

Kinetic Analysis. The initial velocity was measured at 37 °C in 10 min reaction to obtain the enzyme kinetic parameters. The initial velocity for the UDP-glucose substrate was measured at various UDP-glucose concentrations (2.5−60 μM), with the detection probe concentration being fixed at 200 nM. The initial velocity for the 5-hmC-containing substrate DNA (detection probe contains two residues of 5-hmC) was measured at various 5-hmC concentrations (0.02−0.6 μM), with the UDP-glucose concentration being fixed at 80 μM. The kinetic parameter is fitted to the Michaelis−Menten equation.

$$V = \frac{V_{max}[S]}{K_m + [S]} \quad (1)$$

where $[S]$ is the concentration of substrates (UDP-glucose or detection probe), K_m is the substrate concentration for the achievement of half-maximal velocity (i.e., Michaelis−Menten constant), and V_{max} is the maximum initial velocity.

Inhibition Assay. To evaluate the effect of inhibitors (4-phenylimidazole and uridine 5′-diphosphate) upon the activity of β-GT, different concentrations of inhibitors were preincubated with 10 U/mL β-GT at room temperature for 10 min, respectively. Then the premixed solution (1 μL) was incubated with 10 μL of reaction solution containing 200 nM detection probe, 20 mM tris-acetate, 10 mM magnesium acetate, 50 mM potassium acetate, 80 μM UDP-glucose, and

https://dx.doi.org/10.1021/acs.analchem.0c04382
Anal. Chem. XXXX, XXX, XXX−XXX

100 μg/mL BSA, followed by the same detection procedures described above. The relative activity (RA) of β-GT was calculated based on eq 2:

$$\mathrm{RA}(\%) = \frac{F_i - F_0}{F_t - F_0} \times 100\% \quad (2)$$

where F_i is the fluorescence intensity in the presence of different concentrations of inhibitors, F_0 is the measured fluorescence intensity without β-GT, and F_t is the fluorescence intensity in the presence of 1 U/mL β-GT. The IC_{50} value was obtained based on the RA curve versus the inhibitor concentration.

Recovery Assay. Fetal bovine serum (FBS, 1%) was spiked with recombinant β-GT at various concentrations, 200 nM detection probe, 80 μM UDP-glucose, 100 μg/mL BSA, 20 mM tris-acetate,10 mM magnesium acetate, and 50 mM potassium acetate followed by incubation at 37 °C for 1 h. The same detection procedures were used for recovery assay.

RESULTS AND DISCUSSION

Principle of β-GT Biosensor. As illustrated in Scheme 1, a hairpin-structured DNA acts as both a probe for β-GT recognition and a template for HDA amplification. The target β-GT can catalyze the transfer of β-D-glucosyl residue to the hydroxyl group of 5-hmC from UDP-glucose within the MfeI restriction site 5′-^{hm}CAATTG-3′ to form 5-ghmC (Scheme 1A), which efficiently protects the detection probes from MfeI cleavage.[28,46,47] The intact detection probe can survive from Exo III and Exo I treatments due to the phosphonothioate modification at its 3′- and 5′-end. With the addition of helicase, the stem of detection probe is unwound, enabling its hybridization with the primer strand. Subsequently, the primer is extended by DNA polymerase to generate the double-stranded DNA (dsDNA), and each strand can further serve as a new template to trigger another polymerization round. As a result, exponential amplification is achieved, resulting in the production of numerous dsDNAs, which can be detected by dsDNA-specific dye SYBR Green I[48] in a label-free manner. In contrast, when target β-GT is absent, the 5-hmC within the MfeI restriction site is not glucosylated, and the detection probes will be cleaved by MfeI and subsequently completely digested by Exo I and Exo III. As a result, no HDA amplification occurs due to the lack of a template, leading to zero background. Notably, this biosensor enables sensitive, isothermal, and homogenous detection of β-GT without the need of complicated immobilization, washing, and separation steps as well as laborious preparation of functional nanomaterials.

Scheme 1. Schematic Illustration of β-GT-Catalyzed Transfer of β-D-Glucosyl Residue from UDP-Glucose to the Hydroxyl Group of 5-hmC to Form 5-ghmC (A) and the Construction of Fluorescent Biosensor for β-GT Assay (B)

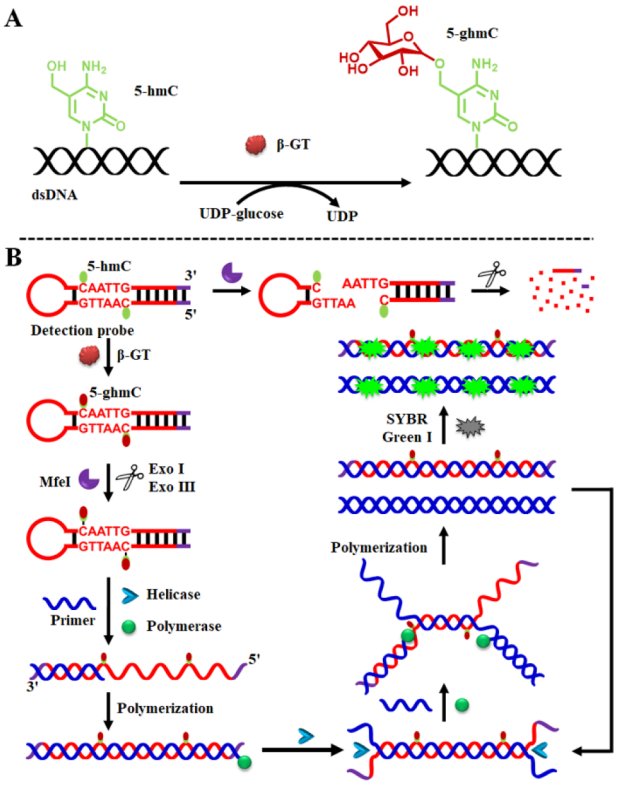

Verification of Assay Feasibility. The 5-hmC glucosylation-mediated protection of detection probes from nuclease digestion is essential for β-GT recognition. We used 12% nondenaturing PAGE to analyze the detection probes after nuclease digestion. When β-GT is present, a band of detection probes can be observed after MfeI, Exo I, and Exo III treatments (Figure 1, lane 1), indicating that β-GT-catalyzed 5-hmC glucosylation may protect the detection probes from nuclease digestion. In contrast, the band of detection probes disappears in the control group without β-GT (Figure 1, lane 2), suggesting the complete digestion of nonglucosylated detection probes by nucleases in the absence of β-GT.

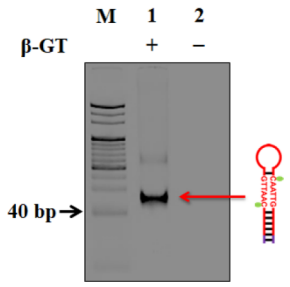

Figure 1. Nondenaturing PAGE (12%) analysis of detection probe digestion. Lane M, 20 bp DNA ladder; lane 1, 100 nM detection probe +10 U/mL β-GT + 10 U of Exo I + 60 U of MfeI +10 U of Exo III; lane 2, 100 nM detection probe +10 U of Exo I + 60 U of MfeI +10 U of Exo III.

The β-GT-induced HDA reaction is confirmed by 2% agarose gel electrophoresis (Figure 2A). When β-GT is present, a band of HDA products is detected (Figure 2A, lane 1), suggesting the occurrence of target-induced HDA reaction. However, no band is observed when β-GT is absent (Figure 2A, lane 2), indicating that no HDA product is produced without β-GT. Meanwhile, the HDA reaction is real-time monitored (Figure 2B). The presence of β-GT induces the rapid increase of fluorescence intensity, with a plateau being reached in 25 min (Figure 2B, red line). In contrast, zero background is detected in the absence of β-GT (Figure 2B, black line). Such zero background can be ascribed to the completed digestion of nonglucosylated detection probes upon nuclease treatment (Figure S1) and efficient elimination of primer−dimer nonspecific amplification via the involvement of

https://dx.doi.org/10.1021/acs.analchem.0c04382
Anal. Chem. XXXX, XXX, XXX−XXX

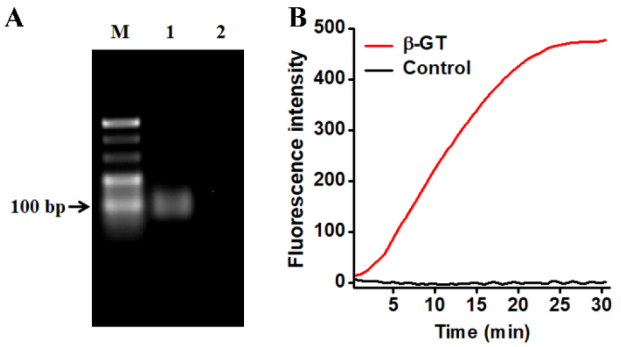

Figure 2. (A) Analysis of HDA products by 2% agarose gel electrophoresis. Lane M, 20 bp DNA ladder; lane 1, 1 U/mL β-GT; lane 2, without β-GT. (B) Real-time monitoring of HDA reaction. Red line, 1 U/mL β-GT; black line (control) without β-GT.

only a single primer.[49] Notably, the glucosylation of HDA template exhibits no significant effect upon the amplification efficiency compared with the nonglucosylated template (Figure S2).

Sensitivity of the β-GT Biosensor. We evaluate the assay sensitivity under the optimized experimental conditions (Figures S1 and S3). When the β-GT concentration increases from 0 to 1 U/mL, the fluorescence intensity enhances monotonically (Figure 3A), indicating that the β-GT concentration is directly proportional to the HDA amplification signal. Moreover, in the logarithm scale, the fluorescence intensity shows a linear correlation with the β-GT concentration in a range of 1×10^{-4}–1 U/mL (Figure 3B). The corresponding equation is $F = 469.03 + 102.25 \log_{10} C$ ($R^2 = 0.9879$), where F represents the fluorescence intensity, and C represents the β-GT concentration (U/mL). The limit of detection (LOD) is calculated to be 2.79×10^{-5} U/mL by calculating the average signal of the blank group plus 3× standard deviation. The sensitivity of this biosensor has been enhanced by 9677-fold and 1434-fold compared with those of the electrochemical method (0.27 U/mL)[30] and electrochemiluminescent method (0.04 U/mL),[32] respectively. The enhanced sensitivity results from (1) specific conversion of β-GT activity signal to amplifiable nucleic acid signal through β-GT-induced 5-hmC glucosylation and (2) highly efficient signal amplification catalyzed by HDA.

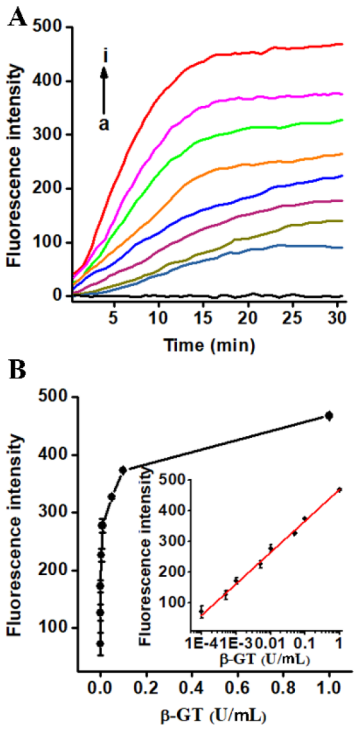

Figure 3. (A) Real-time fluorescence measurement of different concentrations of β-GT (a–i: 0, 1×10^{-4}, 5×10^{-4}, 1×10^{-3}, 0.005, 0.01, 0.05, 0.1, and 1 U/mL). (B) Change of fluorescence intensity induced by different concentrations of β-GT. Inset demonstrates the linear relationship of fluorescence intensity with the β-GT concentration (1×10^{-4}–1 U/mL) in the logarithm scale. Error bars are the standard deviation of three independent experiments.

Specificity of the β-GT Biosensor. The interfering enzymes including uracil DNA glycosylase (UDG), *Hha*I restriction enzyme (*Hha*I), and alkaline phosphatase (ALP) were selected to investigate the assay specificity. *Hha*I can cleave the dsDNA with the recognition sequence 5′-GCGC-3′.[50] UDG is a DNA glycosylase that excises uracil base from DNA.[51] ALP can remove the phosphate groups from the phosphorylated substrates.[52] Theoretically, none of *Hha*I, UDG, ALP, and heat-inactivated β-GT can induce glucosylation of detection probes to protect them from the cleavage and digestion, and thus no isothermal HDA occurs. As expected, no distinct signal is observed in the presence of *Hha*I (Figure 4A, orange column), UDG (Figure 4A, magenta column), ALP (Figure 4A, green column). However, when β-GT is present, a significant high signal is detected (Figure 4A, red column). Moreover, when β-GT is inactivated by heat treatment (Figure 4A, blue column), the fluorescence signal decreases to the same level of the control group (Figure 4A, black column). These results suggest the good specificity of this biosensor toward target β-GT.

To evaluate the substrate specificity, we measured the real-time fluorescence signal induced by C-probe and 5-mC probe in which the 5-hmC base within the detection probe was replaced by C base and 5-mC base, respectively. In the presence of detection probe containing two 5-hmC bases, a significant high fluorescence signal is observed (Figure 4B, red column). However, no distinct signal is observed in response to C-probe (Figure 4B, blue column), 5-mC probe (Figure 4B, green column), and only reaction buffer (Figure 4B, control, black column). Theoretically, C-probe and 5-mC-probe are unable to be glucosylated by β-GT due to the lack of 5-hmC base, and thus these two probes will be completely digested by nucleases, and no HDA occurs.

Kinetic Analysis. For kinetic analysis, the target β-GT was incubated with two β-GT substrates (i.e., UDP-glucose and detection probe) for 10 min at 37 °C, and the initial velocity was measured and plotted against the substrate concentration (Figure 5). The initial velocity enhances with the increase of UDP-glucose concentration from 2.5 to 60 μM (Figure 5A), and the maximal initial velocity (V_{max}) and Michaelis constant (K_m) are calculated to be 35.75 min^{-1} and 8.23 μM, respectively. Moreover, the initial velocity improves with the increase of detection probe concentration from 0.02 to 0.6 μM (Figure 5B), and V_{max} and K_m are measured to be 43.64 min^{-1} and 0.10 μM, respectively. The K_m values obtained by the proposed biosensor are comparable to that obtained by the radioactive assay (16 μM for UDP-glucose and 0.41 μM for DNA substrate, respectively).[28]

https://dx.doi.org/10.1021/acs.analchem.0c04382
Anal. Chem. XXXX, XXX, XXX–XXX

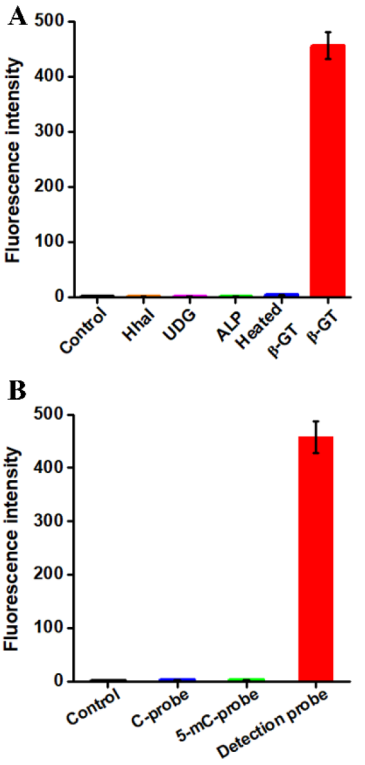

Figure 4. (A) Fluorescence intensity induced by *Hha*I (orange column), UDG (magenta column), ALP (green column), β-GT (red column), heat-inactivated β-GT (blue column), and the control group with only reaction buffer (black column). The concentration of each enzyme is 1 U/mL. (B) Fluorescence intensity induced by C-probe (blue column), 5-mC-probe (green column), detection probe (red column), and the control group (black column). The 200 nM C-probe, 200 nM 5-mC-probe, and 200 nM detection probe were used in the experiments. Error bars are the standard deviation of three independent experiments.

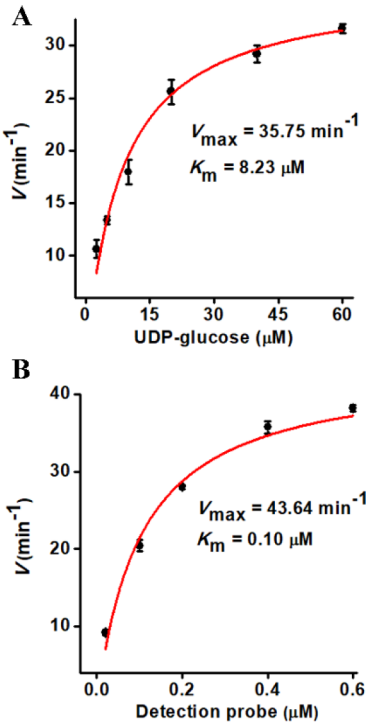

Figure 5. Analysis of Michaelis–Menten kinetic parameters by the initial velocity method using UDP-glucose (A) and detection probe (B). The β-GT concentration is 1 U/mL. Error bars are the standard deviation of three independent experiments.

Inhibition Assay. The 5′-diphosphate and 4-phenylimidazole were used as the model inhibitors[28,53] for β-GT inhibition assay. The relative activity of β-GT gradually decreases with the increase of uridine 5′-diphosphate concentration in a range of 1–50 μM (Figure 6A). The IC_{50} value (i.e., the inhibitor concentration for reducing the β-GT activity by 50%) is measured to be 10.12 μM, consistent with that obtained by gold nanocluster-based electrochemiluminescent method (13.54 μM).[33] Moreover, the relative activity of β-GT decreases with the increase of 4-phenylimidazole concentration in a dose-dependent manner in a range of 1–10 μM (Figure 6B). The IC_{50} value is measured to be 3.51 μM, consistent with that obtained by the gold nanoparticle-based electrochemiluminescent method (4.75 μM).[32] These results suggest the great potential of this biosensor in β-GT-targeted antiviral and antiparasitic drug discovery.

Real Sample Analysis. To demonstrate the proof-of-concept of real sample analysis, we carried out the recovery studies by spiking varying concentrations of β-GT (0.1, 0.5, and 1 U/mL) into 1% fetal bovine serum samples. The recovery ratio is measured to be 99.84–100.36% with a relative standard deviation (RSD) of 0.70–1.03% (Table 2), demonstrating the good assay performance of this biosensor in the complex biological matrix.

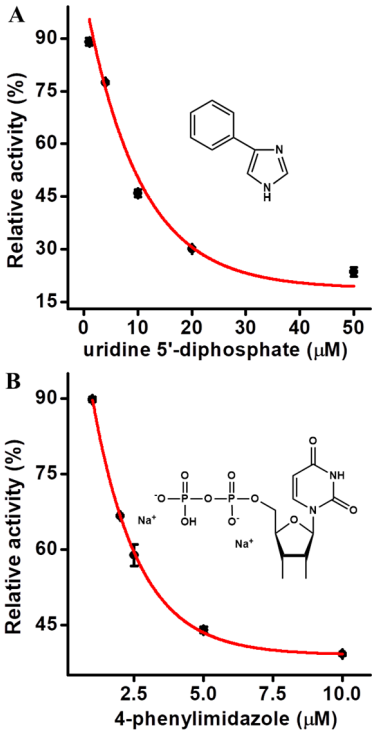

Figure 6. Inhibition effects of uridine 5′-diphosphate (A) and 4-phenylimidazole (B) upon the β-GT activity. The β-GT concentration is 10 U/mL. Error bars are the standard deviation of three independent experiments.

https://dx.doi.org/10.1021/acs.analchem.0c04382
Anal. Chem. XXXX, XXX, XXX–XXX

Table 2. Recovery of β-GT Spiked in Serum Samples

added (U/mL)	measured (U/mL)	recovery (%)	RSD (%)
1.00	1.010	100.09	0.70
0.50	0.518	100.36	0.72
0.10	0.099	99.84	1.03

CONCLUSIONS

We demonstrate the development of a new sensitive fluorescent biosensor for selective detection of β-GT activity with zero background signal. In this biosensor, the β-GT-catalyzed 5-hmC glucosylation protects the detection probes from MfeI-mediated cleavage and Exo III/Exo I-mediated digestion, and the remaining detection probes consequently trigger HDA to produce an amplified fluorescence signal. This biosensor possesses some significant advantages: (1) because only a single primer is involved, the primer−dimer nonspecific amplification can be efficiently eliminated;[49] due to the completed digestion of nonglucosylated detection probes by nuclease treatment, zero background can be obtained. (2) The integration of HAD-mediated signal amplification with zero background enables the achievement of high sensitivity with over three orders of magnitude improvement than the reported β-GT assays.[30,32] (3) This biosensor is simple, isothermal, and homogenous without the involvement of complicated immobilization, separation, and washing steps.[27,29−33] (4) The signal can be simply monitored in a label-free manner, avoiding the laborious preparation and functionalization of nanomaterials.[30−33] In addition, this biosensor can be used for inhibitor screening, β-GT kinetic analysis, and accurate β-GT detection in complex biological samples, providing a promising platform for better revealing β-GT fundamental biological functions and promoting related epigenetic researches. Importantly, this biosensor can be extended to detect various DNA-modifying enzymes by replacing the recognition sequence in the detection probe and using the corresponding restriction enzyme.

ASSOCIATED CONTENT

Supporting Information

The Supporting Information is available free of charge at https://pubs.acs.org/doi/10.1021/acs.analchem.0c04382.

Influence of exonuclease concentration upon background signal, effect of detection probe glucosylation upon the HDA amplification, and effect of β-GT incubation time upon the assay performance (PDF)

AUTHOR INFORMATION

Corresponding Authors

Xiliang Luo − *Key Laboratory of Optic-electric Sensing and Analytical Chemistry for Life Science, MOE; Shandong Key Laboratory of Biochemical Analysis; Key Laboratory of Analytical Chemistry for Life Science in Universities of Shandong; and College of Chemistry and Molecular Engineering, Qingdao University of Science and Technology, Qingdao 266042, P. R. China;* orcid.org/0000-0001-6075-7089; Email: xiliangluo@qust.edu.cn

Fei Ma − *College of Chemistry, Chemical Engineering and Materials Science, Collaborative Innovation Center of Functionalized Probes for Chemical Imaging in Universities of Shandong, Key Laboratory of Molecular and Nano Probes, Ministry of Education, Shandong Provincial Key Laboratory of Clean Production of Fine Chemicals, Shandong Normal University, Jinan 250014, China;* Email: flyma100@163.com

Chun-yang Zhang − *College of Chemistry, Chemical Engineering and Materials Science, Collaborative Innovation Center of Functionalized Probes for Chemical Imaging in Universities of Shandong, Key Laboratory of Molecular and Nano Probes, Ministry of Education, Shandong Provincial Key Laboratory of Clean Production of Fine Chemicals, Shandong Normal University, Jinan 250014, China;* orcid.org/0000-0002-8010-1981; Phone: +86 0531-86186033; Email: cyzhang@sdnu.edu.cn; Fax: : +86 0531-82615258

Authors

Meng Liu − *College of Chemistry, Chemical Engineering and Materials Science, Collaborative Innovation Center of Functionalized Probes for Chemical Imaging in Universities of Shandong, Key Laboratory of Molecular and Nano Probes, Ministry of Education, Shandong Provincial Key Laboratory of Clean Production of Fine Chemicals, Shandong Normal University, Jinan 250014, China*

Chen-chen Li − *College of Chemistry, Chemical Engineering and Materials Science, Collaborative Innovation Center of Functionalized Probes for Chemical Imaging in Universities of Shandong, Key Laboratory of Molecular and Nano Probes, Ministry of Education, Shandong Provincial Key Laboratory of Clean Production of Fine Chemicals, Shandong Normal University, Jinan 250014, China; Key Laboratory of Optic-electric Sensing and Analytical Chemistry for Life Science, MOE; Shandong Key Laboratory of Biochemical Analysis; Key Laboratory of Analytical Chemistry for Life Science in Universities of Shandong; and College of Chemistry and Molecular Engineering, Qingdao University of Science and Technology, Qingdao 266042, P. R. China*

Complete contact information is available at: https://pubs.acs.org/10.1021/acs.analchem.0c04382

Author Contributions

‡M.L. and C.-C.L.. contributed equally.

Notes

The authors declare no competing financial interest.

ACKNOWLEDGMENTS

This work was supported by the National Natural Science Foundation of China (grant nos. 21735003, 21527811, and 21705096), the Taishan Scholar Program of Shandong Province of China (ts20110829), and the Award for Team Leader Program of Taishan Scholars of Shandong Province, China.

REFERENCES

(1) Sukovich, D. J.; Modavi, C.; de Raad, M.; Prince, R. N.; Anderson, J. C. *ACS Synth. Biol.* **2015**, *4*, 833−841.
(2) Volkin, E. *J. Am. Chem. Soc.* **1954**, *76*, 5892−5893.
(3) Josse, J.; Kornberg, A. *J. Biol. Chem.* **1962**, *237*, 1968−1976.
(4) Booth, M. J.; Raiber, E.-A.; Balasubramanian, S. *Chem. Rev.* **2015**, *115*, 2240−2254.
(5) Zheng, Y.; Cohen-Karni, D.; Xu, D.; Chin, H. G.; Wilson, G.; Pradhan, S.; Roberts, R. J. *Nucleic Acids Res.* **2010**, *38*, 5527−5534.
(6) Wang, H.; Guan, S.; Quimby, A.; Cohen-Karni, D.; Pradhan, S.; Wilson, G.; Roberts, R. J.; Zhu, Z.; Zheng, Y. *Nucleic Acids Res.* **2011**, *39*, 9294−9305.

(7) Cox, G. S.; Conway, T. W. *J. Virol.* **1973**, *12*, 1279−1287.
(8) Borst, P.; Fairlamb, A. H. *Annu. Rev. Microbiol.* **1998**, *52*, 745−778.
(9) Münzel, M.; Globisch, D.; Carell, T. *Angew. Chem. Int. Ed.* **2011**, *50*, 6460−6468.
(10) Nabel, C. S.; Kohli, R. M. *Science* **2011**, *333*, 1229−1230.
(11) Nawy, T. *Nat. Methods* **2013**, *10*, 466−466.
(12) Gao, Y.; Chen, J.; Li, K.; Wu, T.; Huang, B.; Liu, W.; Kou, X.; Zhang, Y.; Huang, H.; Jiang, Y.; Yao, C.; Liu, X.; Lu, Z.; Xu, Z.; Kang, L.; Chen, J.; Wang, H.; Cai, T.; Gao, S. *Cell Stem Cell* **2013**, *12*, 453−469.
(13) Ficz, G.; Branco, M. R.; Seisenberger, S.; Santos, F.; Krueger, F.; Hore, T. A.; Marques, C. J.; Andrews, S.; Reik, W. *Nature* **2011**, *473*, 398−402.
(14) Koh, K. P.; Yabuuchi, A.; Rao, S.; Huang, Y.; Cunniff, K.; Nardone, J.; Laiho, A.; Tahiliani, M.; Sommer, C. A.; Mostoslavsky, G.; Lahesmaa, R.; Orkin, S. H.; Rodig, S. J.; Daley, G. Q.; Rao, A. *Cell Stem Cell* **2011**, *8*, 200−213.
(15) Tan, L.; Shi, Y. G. *Development* **2012**, *139*, 1895−1902.
(16) Branco, M. R.; Ficz, G.; Reik, W. *Nat. Rev. Genet.* **2012**, *13*, 7−13.
(17) Mastroeni, D.; Grover, A.; Delvaux, E.; Whiteside, C.; Coleman, P. D.; Rogers, J. *Neurobiol. Aging* **2010**, *31*, 2025−2037.
(18) Tahiliani, M.; Koh, K. P.; Shen, Y.; Pastor, W. A.; Bandukwala, H.; Brudno, Y.; Agarwal, S.; Iyer, L. M.; Liu, D. R.; Aravind, L.; Rao, A. *Science* **2009**, *324*, 930−935.
(19) Jin, S.-G.; Jiang, Y.; Qiu, R.; Rauch, T. A.; Wang, Y.; Schackert, G.; Krex, D.; Lu, Q.; Pfeifer, G. P. *Cancer Res.* **2011**, *71*, 7360−7365.
(20) Lian, C. G.; Xu, Y.; Ceol, C.; Wu, F.; Larson, A.; Dresser, K.; Xu, W.; Tan, L.; Hu, Y.; Zhan, Q.; Lee, C.-w.; Hu, D.; Lian, B. Q.; Kleffel, S.; Yang, Y.; Neiswender, J.; Khorasani, A. J.; Fang, R.; Lezcano, C.; Duncan, L. M.; Scolyer, R. A.; Hompson, J. F.; Kakavand, T. H.; Houvras, Y.; Zon, L. I.; Mihm, M. C., Jr.; Kaiser, U. B.; Schatton, T.; Woda, B. A.; Murphy, G. F.; Shi, Y. G. *Cell* **2012**, *150*, 1135−1146.
(21) Yang, H.; Liu, Y.; Bai, F.; Zhang, J. Y.; Ma, S. H.; Liu, J.; Xu, Z. D.; Zhu, H. G.; Ling, Z. Q.; Ye, D.; Guan, K. L.; Xiong, Y. *Oncogene* **2013**, *32*, 663−669.
(22) Liu, Y.; Siejka-Zielińska, P.; Velikova, G.; Bi, Y.; Yuan, F.; Tomkova, M.; Bai, C.; Chen, L.; Schuster-Böckler, B.; Song, C.-X. *Nat. Biotechnol.* **2019**, *37*, 424−429.
(23) Povedano, E.; Ruiz-Valdepeñas Montiel, V.; Gamella, M.; Pedrero, M.; Barderas, R.; Peláez-García, A.; Mendiola, M.; Hardisson, D.; Feliú, J.; Yáñez-Sedeño, P.; Campuzano, S.; Pingarrón, J. M. *Anal. Chem.* **2020**, *92*, 5604−5612.
(24) Robertson, A. B.; Dahl, J. A.; Vågbø, C. B.; Tripathi, P.; Krokan, H. E.; Klungland, A. *Nucleic Acids Res.* **2011**, *39*, e55−e55.
(25) Song, C.-X.; Szulwach, K. E.; Fu, Y.; Dai, Q.; Yi, C.; Li, X.; Li, Y.; Chen, C.-H.; Zhang, W.; Jian, X.; Wang, J.; Zhang, L.; Looney, T. J.; Zhang, B.; Godley, L. A.; Hicks, L. M.; Lahn, B. T.; Jin, P.; He, C. *Nat. Biotechnol.* **2011**, *29*, 68−72.
(26) Song, C.-X.; Diao, J.; Brunger, A. T.; Quake, S. R. *P. Natl. Acad. Sci. U.S.A.* **2016**, *113*, 4338−4343.
(27) Moréra, S.; Imberty, A.; Aschke-Sonnenborn, U.; Rüger, W.; Freemont, P. S. *J. Mol. Biol.* **1999**, *292*, 717−730.
(28) Terragni, J.; Bitinaite, J.; Zheng, Y.; Pradhan, S. *Biochemistry* **2012**, *51*, 1009−1019.
(29) Zhou, Y.; Yang, Z.; Li, X.; Wang, Y.; Yin, H.; Ai, S. *Electrochim. Acta* **2015**, *174*, 647−652.
(30) Yin, H.; Yang, Z.; Wang, H.; Zhou, Y.; Ai, S. *Sens. Actuators, B* **2017**, *243*, 602−608.
(31) Sui, C.; Wang, T.; Zhou, Y.; Yin, H.; Meng, X.; Zhang, S.; Waterhouse, G. I. N.; Xu, Q.; Zhuge, Y.; Ai, S. *Biosens. Bioelectron.* **2019**, *127*, 38−44.
(32) Sun, H.; Ma, S.; Li, Y.; Qi, H.; Ning, X.; Zheng, J. *Biosens. Bioelectron.* **2016**, *79*, 92−97.
(33) Jiang, W.; Yin, H.; Zhou, Y.; Duan, J.; Li, H.; Wang, M.; Waterhouse, G. I. N.; Ai, S. *Sens.. Actuators, B* **2018**, *274*, 144−151.
(34) Zhao, Y.; Chen, F.; Li, Q.; Wang, L.; Fan, C. *Chem. Rev.* **2015**, *115*, 12491−12545.
(35) Vincent, M.; Xu, Y.; Kong, H. *EMBO Rep.* **2004**, *5*, 795−800.
(36) Ho, S. N.; Hunt, H. D.; Horton, R. M.; Pullen, J. K.; Pease, L. R. *Gene* **1989**, *77*, 51−59.
(37) Ma, F.; Yang, Y.; Zhang, C.-y. *Anal. Chem.* **2014**, *86*, 6006−6011.
(38) Zhou, L.; Ou, L.-J.; Chu, X.; Shen, G.-L.; Yu, R.-Q. *Anal. Chem.* **2007**, *79*, 7492−7500.
(39) Li, D.; Zhang, T.; Yang, F.; Yuan, R.; Xiang, Y. *Anal. Chem.* **2020**, *92*, 2074−2079.
(40) Notomi, T.; Okayama, H.; Masubuchi, H.; Yonekawa, T.; Watanabe, K.; Amino, N.; Hase, T. *Nucleic Acids Res.* **2000**, *28*, e63−e663.
(41) Scott, A. T.; Layne, T. R.; O'Connell, K. C.; Tanner, N. A.; Landers, J. P. *Anal. Chem.* **2020**, *92*, 13343−13353.
(42) Jeong, Y.-J.; Park, K.; Kim, D.-E. *Cell. Mol. Life Sci.* **2009**, *66*, 3325.
(43) Ma, F.; Liu, M.; Tang, B.; Zhang, C.-y. *Anal. Chem.* **2017**, *89*, 6182−6187.
(44) Cao, A.; Zhang, C.-y. *Anal. Chem.* **2013**, *85*, 2543−2547.
(45) Andresen, D.; von Nickisch-Rosenegk, M.; Bier, F. F. *Clin. Chim. Acta* **2009**, *403*, 244−248.
(46) Schübeler, D. *Nature* **2015**, *517*, 321−326.
(47) Kinney, S. M.; Chin, H. G.; Vaisvila, R.; Bitinaite, J.; Zheng, Y.; Estève, P.-O.; Feng, S.; Stroud, H.; Jacobsen, S. E.; Pradhan, S. *J. Biol. Chem.* **2011**, *286*, 24685−24693.
(48) He, J.-L.; Wu, Z.-S.; Zhou, H.; Wang, H.-Q.; Jiang, J.-H.; Shen, G.-L.; Yu, R.-Q. *Anal. Chem.* **2010**, *82*, 1358−1364.
(49) Chen, F.; Zhang, D.; Zhang, Q.; Zuo, X.; Fan, C.; Zhao, Y. *ChemBioChem* **2016**, *17*, 1171−1176.
(50) Roberts, R. J.; Myers, P. A.; Morrison, A.; Murray, K. *J. Mol. Biol.* **1976**, *103*, 199−208.
(51) Wang, L.-j.; Ren, M.; Zhang, Q.; Tang, B.; Zhang, C.-y. *Anal. Chem.* **2017**, *89*, 4488−4494.
(52) Ma, F.; Liu, W.-j.; Liang, L.; Tang, B.; Zhang, C.-Y. *Chem. Commun.* **2018**, *54*, 2413−2416.
(53) Li, Y.-K.; Byers, L. D. *BBA-Protein Struct. M.* **1989**, *999*, 227−232.

https://dx.doi.org/10.1021/acs.analchem.0c04382
Anal. Chem. XXXX, XXX, XXX−XXX